Department of Pharmaceutics, Faculty of Pharmacy, Osaka Medical and Pharmaceutical University, Osaka, Japan

Internalization of FITC-albumin in human adipose-derived stem cells: Involvement of clathrin and caveolin

Hongxin Sun, Yumiko Urakami-Takebayashi, Hideyuki Motohashi, Junya Nagai*

Received February 17, 2022, accepted March 22, 2022

**Corresponding author: Junya Nagai, Department of Pharmaceutics, Faculty of Pharmacy, Osaka Medical and Pharmaceutical University, 4-20-1 Nasahara, Takatsuki, Osaka 569-1094, Japan.*
junya.nagai@ompu.ac.jp

Pharmazie 77: 141-146 (2022) *doi: 10.1691/ph.2022.2340*

Adipose tissue-derived stem cells (AdSCs) are one of the most promising cell types for cell-based therapies. In addition, AdSCs systematically injected into the body have been reported to localize to damaged tissues and certain types of tumor. As an important part of establishing a potent drug delivery system with AdSCs, the mechanism and efficiency of uptake into AdSCs has drawn much research attention. However, this remains to be fully clarified. The aim of this study was to examine the characteristics of endocytosis-mediated uptake in human AdSCs. We used fluorescein isothiocyanate-labeled albumin (FITC-albumin) as a potent marker of endocytosis. FITC-albumin uptake was time- and temperature-dependent. Confocal microscopy showed punctate localization of fluorescence in the cytoplasm. FITC-albumin uptake was inhibited by human serum albumin in a concentration-dependent manner. FITC-albumin uptake was inhibited by a metabolic inhibitor (2,4-dinitrophenol), a microtubule polymerization inhibitor (colchicine), an actin polymerization inhibitor (cytochalasin D), endosomal acidification inhibitors (chloroquine and bafilomycin A_1), clathrin-dependent endocytosis inhibitors (chloropromazine, phenylarsine oxide, and Pitstop2), and caveolin-dependent endocytosis inhibitors (nystatin and methyl-β-cyclodextrin). Furthermore, the knockdown of the clathrin heavy chain and caveolin-1 significantly reduced FITC-albumin uptake. These findings suggest that AdSCs take up albumin via endocytic pathways in which clathrin and caveolin are involved.

1. Introduction

Stem cell therapy is one of the most promising medications for the treatment of many conditions, including neurodegenerative disorders, cardiac diseases, immunological diseases, and bone defects. Stem cells are useful in organ and tissue reconstruction due to their ability to be abundantly harvested by minimally invasive methods, as well as their ability to differentiate into multiple cell lineages. Stem cell candidates include embryonic stem cells, induced pluripotent stem cells, and adult stem cells, such as mesenchymal stem cells (MSCs). However, concerns regarding the use of embryonic stem cells are common, particularly ethical concerns and in terms of immune responses. Induced pluripotent stem cells are an alternative that allows researchers to avoid these ethical concerns and immune responses. However, the cell preparation method associated these cells is relatively complex (Lindvall et al. 2004; Segers and Lee 2008; Zhang et al. 2020).

MSCs were first isolated from the bone marrow as part of the stroma, which supports the maturation of hematopoietic cells. MSCs are not only found in the bone marrow but also in a range of tissues, including in adipose-derived stem cells, umbilical cord blood, synovium, and skeletal muscle. MSCs have been reported to differentiate into vascular endothelial cells, osteoblasts, chondrocytes, and adipocytes. The harvesting of bone marrow requires an invasive procedure that yields a small number of cells. In addition, the number, differentiation potential, and lifespan of MSCs from bone marrow decline with patient age, suggesting an inverse relationship between stem cell potential and donor age (Zhang et al. 2020; Kunze et al. 2020; Lin et al. 2006; Strem et al. 2005).

Adipose-derived stem cells (AdSCs) were first isolated from white adipose tissue, as reported by Zuk et al. (2001 and 2002). Adipose tissue obtained from subcutaneous tissue represents the most abundant potential source for harvesting AdSCs. In addition, higher yields of AdSCs can easily be obtained from subcutaneous regions through a minimally invasive and painless procedure. The cellular yield of AdSCs is more than 1,000-fold higher than that of MSCs from the bone marrow and umbilical cord blood. The expansion potential, differentiation capacity, and immunophenotype of AdSCs were similar to those of bone marrow-derived MSCs (Kern et al. 2006, Scioli et al. 2019). AdSCs reportedly release a variety of paracrine factors and extracellular vesicles, allowing them to repair damaged tissues. These advantages make AdSCs one of the most attractive resources for use in regenerative medicine.

Moreover, MSCs have been reported to reach damaged tissues and tumor sites from distant body areas via systemic circulation (Shah 2012; Chulpanova et al. 2018; Gao et al. 2013). The targeting capacity makes MSCs a suitable carrier for the delivery of anti-neoplastic and anti-inflammatory drugs. The approach with drug-loaded MSCs could be a more effective and safer therapy by reaching higher local concentrations and minimizing systematic adverse drug effects. However, the mechanism and factors responsible for the targeted tropism of MSCs to wounds and tumor microenvironment remain unclear.

The mechanism and efficiency of drug uptake into cells have drawn much attention due to their importance in establishing a cell-type carrier as a drug delivery device. Hsu et al. (2012) reported that iron oxide nanoparticles and plasmid DNA were taken up primarily by clathrin- and caveolin-mediated endocytosis in rat AdSCs. Yang et al. (2017) suggested that both clathrin-mediated endocytosis and phagocytosis are involved in the uptake of magnetic nanoparticles in rat AdSCs. Endocytosis can be generally divided into macropinocytosis, clathrin-dependent endocytosis, caveolin-dependent endocytosis, and clathrin/caveolin-independent endocytosis (Miaczynska and Stenmark 2008; Conner and Schmid 2003). However, the characterization of endocytosis in AdSCs, especially from human adipose tissue, remains to be clarified. In this study, we investigated the molecular mechanism

underlying the accumulation of a high molecular weight protein in human adipose-derived stem cells (hAdSCs) using fluorescein isothiocyanate-labeled albumin (FITC-albumin) as an endocytosis marker protein.

2. Investigations and results

2.1. Effect of temperature on FITC-albumin uptake in hAdSCs

We first examined the temperature dependence of the uptake of FITC-albumin by hAdSCs (Fig. 1). The uptake of FITC-albumin at 37°C increased with an increasing incubation time, but was modest at 4°C. In addition, the uptake of FITC-albumin was significantly higher at 37°C than at 4°C at all of the incubation times examined. Next, the intracellular localization of FITC-albumin at 37°C and 4°C was examined by confocal laser scanning microscopy (Fig. 2). When hAdSCs were incubated with FITC-albumin at 37°C for 60 min, fluorescence was detected in the cells, and the cells exhibited a punctate pattern. In contrast, a very faint fluorescence was observed when hAdSCs were incubated at 4°C.

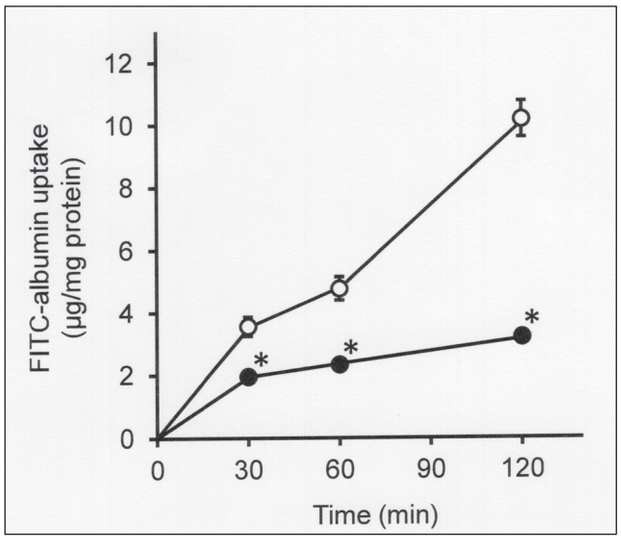

Fig. 1: Time and temperature dependence of fluorescein isothiocyanate-labeled albumin (FITC-albumin) uptake by human adipose-derived stem cells (hAdSCs). The uptake of FITC-albumin (100 μg/ml) by hAdSCs was measured at 37°C (open circles) or 4°C (closed circles). Each point represents the mean ± S.E. of four determinants. *P < 0.05, significantly different compared with the value at each incubation time at 37°C.

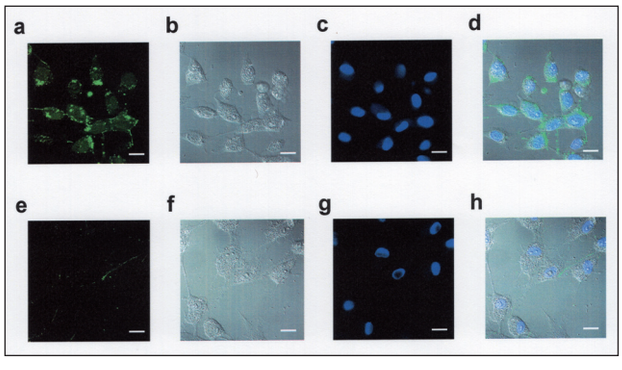

Fig. 2: Confocal laser scanning micrographs of hAdSCs treated with FITC-albumin. After incubation with FITC-albumin (300 μg/ml) at 37°C (a, b, c, and d) or 4°C (e, f, g, and h) for 2 h with 10 μM Hoechst33342 for 60 min, the cells were then observed using confocal laser scanning microscopy. (a, e) FITC-albumin (green), (b, f) differential interference contrast, (c, g) Hoechst33342 (blue), and (d, h) merge. Scale bar, 20 μm.

2.2. Concentration-dependent effect on FITC-albumin uptake

To investigate the involvement of receptor molecule(s) in the uptake of FITC-albumin by hAdSCs, we first examined the effect of unlabeled human serum albumin on FITC-albumin uptake in hAdSCs. Albumin from human serum inhibited FITC-albumin uptake in hAdSCs in a concentration-dependent manner (Fig. 3). The estimated IC_{50} value of human serum albumin was 3.39 mg/ml.

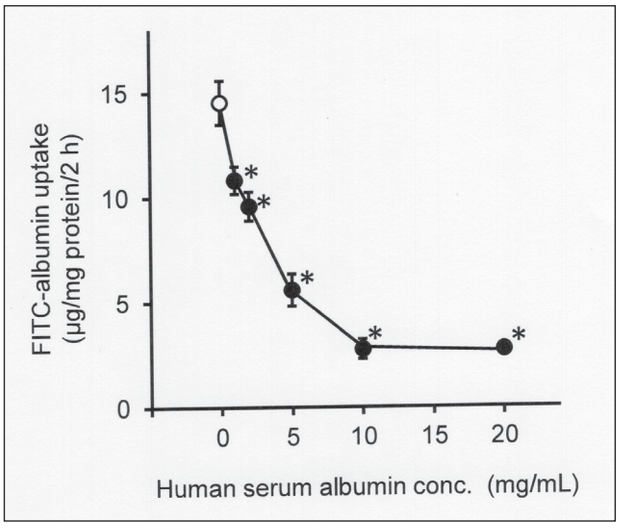

Fig. 3: Effect of human serum albumin on FITC-albumin in hAdSCs. The uptake of FITC-albumin (300 μg/ml) in the absence (open circle) or presence (closed circle) of various concentrations of human serum albumin was measured at 37°C for 2 h. Each point represents the mean ± S.E. of four determinants. *P < 0.05, significantly different from the value in the absence of human serum albumin.

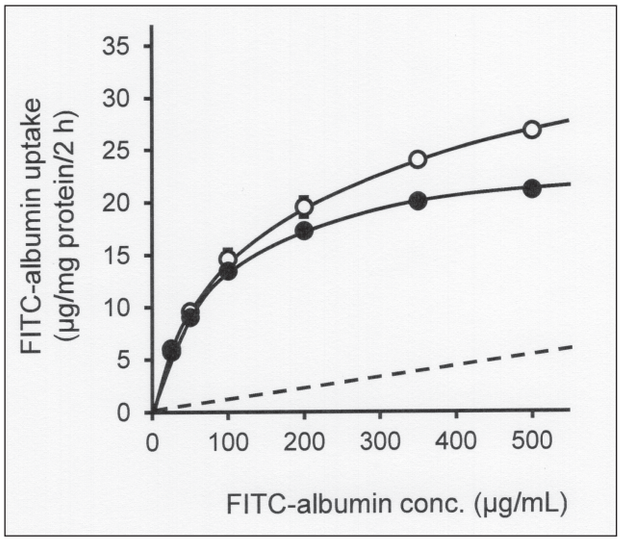

Fig. 4: Concentration dependence of FITC-albumin uptake by hAdSCs. The uptake of various concentrations of FITC-albumin by hAdSCs was measured at 37°C for 2 h. Open circles and dashed lines indicate the total uptake and the calculated value of non-saturable uptake, respectively. The closed circle shows the saturable uptake, which was calculated by subtracting the non-saturable uptake from the total uptake at each FITC-albumin concentration. Each point represents the mean ± S.E. of four determinants.

Figure 4 shows the concentration dependence of FITC-albumin uptake by hAdSCs. The relationship between the concentration and the uptake rate of FITC-albumin was nonlinear, indicating the involvement of a saturable process in the entry of FITC-albumin into hAdSCs. The kinetic parameters were calculated as described

in the Materials and Methods section. The K_m, V_{max}, and K_d were estimated to be 85.1 µg/mL, 24.8 µg/mg protein per 2 h and 0.0112 mL/mg of protein per 2 h, respectively.

2.3. *Effects of various inhibitors of endocytosis on FITC-albumin uptake*

The effects of various chemical endocytosis inhibitors on FITC-albumin uptake were examined to characterize the molecular mechanisms underlying the internalization of FITC-albumin in hAdSCs (Table). The metabolic inhibitor 2,4-dinitrophenol, an uncoupler of oxidative phosphorylation, significantly decreased the uptake of FITC-albumin, indicating that the internalization of FITC-albumin is dependent on metabolic energy. The microtubule polymerization inhibitor colchicine and the actin polymerization inhibitor cytochalasin D significantly decreased the uptake of FITC-albumin. FITC-albumin uptake was inhibited by bafilomycin A_1 and chloroquine, two inhibitors of endosomal acidification, which plays an important role in the dissociation of ligands from receptors in receptor-mediated endocytosis. Next, we examined the effects of clathrin-dependent inhibitors (chloropromazine, phenylarsine oxide, and Pitstop2) and caveolin-dependent endocytosis inhibitors (nystatin and methyl-β-cyclodextrin) on the uptake of FITC-albumin. These inhibitors significantly decreased FITC-albumin uptake. Furthermore, the effect of hypertonicity, which disrupts clathrin-coated pit formation, was examined in terms of FITC-albumin uptake. A high concentration of sucrose (400 mM) significantly reduced FITC-albumin uptake (16.6 ± 0.4% of control; n = 6). In addition, the uptake of FITC-albumin was inhibited by dynasore, an inhibitor of dynamin, which is essential for membrane fission during endocytosis.

Table: Effects of various chemical inhibitors on FITC-albumin uptake by hAdSCs.

	FITC-albumin uptake in hAdSCs (% of control)
Metabolic inhibitor	
1 mM 2,4-dinitrophenol	31.8 ± 1.4*
Microtubule polymerization inhibitor	
50 µM colchicine	21.0 ± 1.5*
Actin polymerization inhibitor	
5 µM cytochalasin D	28.2 ± 0.6*
Endosomal acidification inhibitor	
100 µM chloroquine	28.2 ± 0.6*
1.6 µM bafilomycin A_1	34.4 ± 1.9*
Clathrin-dependent endocytosis inhibitor	
50 µM chloropromazine	27.8 ± 0.3*
10 µM phenylarsine oxide	22.0 ± 0.7*
30 µM Pitstop2	33.5 ± 2.9*
Caveolin-dependent endocytosis inhibitor	
50 µg/ml nystatin	24.2 ± 2.1*
10 mM methyl-β-cyclodextrin	41.1 ± 2.0*
Dynamin inhibitor	
80 µM dynasore	48.5 ± 0.5*

The uptake of FITC-albumin (100 µg/ml) by hAdSCs treated with each inhibitor or its vehicle (control) was measured at 37°C for 2 h. Each point represents the mean ± S.E. of four to six determinants. *P < 0.05, significantly different compared with each control.

2.4. *Expression and cellular localization of clathrin and caveolin in hAdSCs*

To further clarify the involvement of clathrin and caveolin in the internalization of FITC-albumin into hAdSCs, the expression of clathrin and caveolin-1 in hAdSCs was examined by immunoblotting (Fig. 5a). With antibodies raised against clathrin heavy chain and caveolin-1, each protein (with an apparent molecular weight mass of approximately 180 kDa and 21 kDa, respectively) was detected in the cell lysate from hAdSCs.

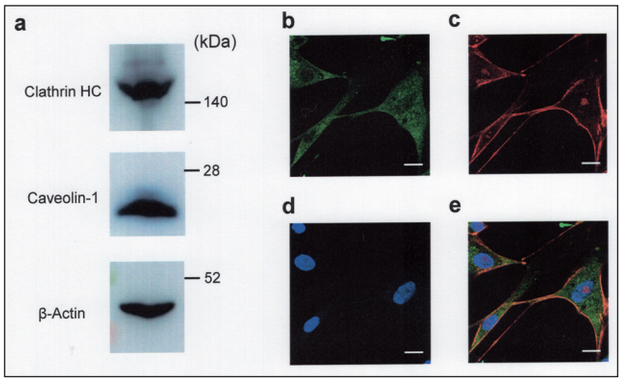

Fig. 5: Western blot analysis of clathrin heavy chain (HC) and caveolin-1 in hAdSCs lysate and confocal laser scanning microscopy analysis of clathrin HC and caveolin-1 localization in hAdSCs. (a) The lysate of hAdSCs was separated in SDS-polyacrylamide gel electrophoresis and transferred to a polyvinylidene difluoride membrane. Clathrin HC, caveolin-1, and β-actin was detected by western blotting. Immunofluorescent localization of clathrin heavy chain (green) (b) and caveolin-1 (red) (c). Nuclei were stained with Hoechst33342 (blue). (d) Merged images. Scale bar, 20 µm.

Next, the cellular localization of clathrin and caveolin-1 in hAdSCs was examined by immunofluorescence confocal microscopy (Fig. 5b). Clathrin was found in a punctate pattern in the cytoplasm, whereas caveolin-1 was strongly detected in the cell membrane. In addition, the fluorescence of caveolin-1 was observed at certain spots on the nuclei.

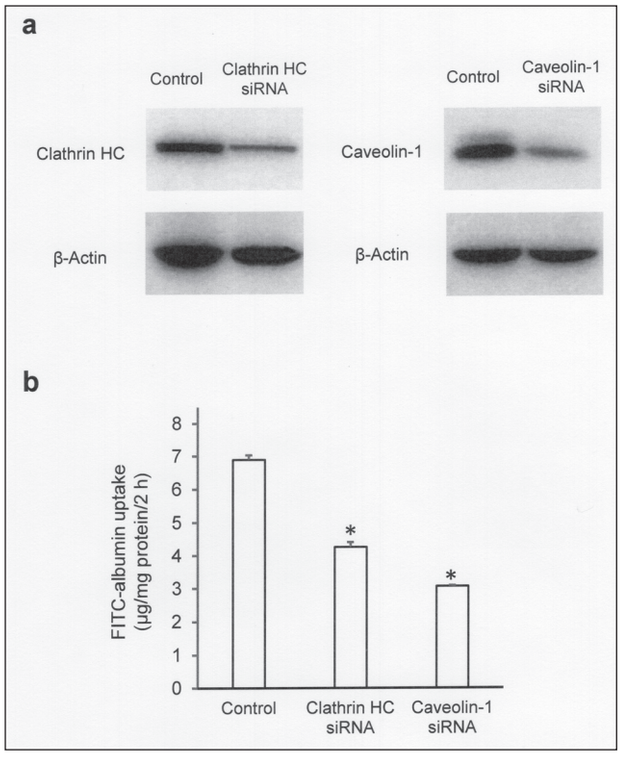

Fig. 6: Effect of clathrin heavy chain (HC) and caveolin-1 knockdown on FITC-albumin uptake by hAdSCs. hAdSCs were transfected without or with clathrin HC and caveolin-1 siRNA for 4 h. After 48 h post transfection, the cells were used for uptake study and western blotting. (a) Immunoblotting for clathrin HC and caveolin-1 in control and siRNA-transfected cells. (b) The uptake of FITC-albumin (100 µg/ml) in control and siRNA-transfected cells was measured at 37°C for 2 h. Each point represents the mean ± S.E. of four determinants. *P < 0.05, significantly different compared with the control.

2.5. Effects of clathrin and caveolin-1 knockdown on FITC-albumin uptake in hAdSCs

We analyzed the role of clathrin and caveolin in the internalization of FITC-albumin by hAdSCs using the RNA interference (RNAi)-mediated knockdown method. As shown in Fig. 6a, immunoblot analysis revealed that the transfection of siRNA duplexes for each target mRNA into hAdSCs decreased the expression of clathrin heavy chain and caveolin-1, but not β-actin. With a decrease in the expression of clathrin heavy chain and caveolin-1, the siRNA repression of clathrin heavy chain and caveolin-1 significantly reduced the uptake of FITC-albumin (Fig. 6b).

3. Discussion

In this study, we characterized the uptake of FITC-albumin in hAdSCs to clarify the endocytosis mechanism in hAdSCs. The cellular uptake mechanisms of albumin have been reported in cultured cells from various tissues. Schwegler et al. showed that FITC-albumin was taken up by receptor-mediated endocytosis in the opossum kidney cell line (Schwegler et al. 1991), which has characteristics similar to those of proximal tubular epithelial cells. Yumoto et al. (2006) reported that FITC-albumin uptake is mediated by endocytosis in the alveolar type II epithelial cell line RLE-6TN. Dobrinskikh et al. (2014) suggested that podocytes can endocytose albumin by examining the uptake mechanism of FITC-albumin in cultured human urine-derived podocyte-like epithelial cells. In accordance with these previous reports, the uptake of FITC-albumin in hAdSCs was markedly decreased at 4°C compared to 37°C. Considering that the molecular size of albumin is approximately 66 kDa, we postulated that the cellular entry of FITC-albumin in hAdSCs was due to endocytosis rather than movement across the cell membrane, such as simple diffusion and transporter-mediated transport.

The inhibitory effect of human serum albumin on FITC-albumin uptake in hAdSCs indicated that both FITC-labeled albumin (from bovine serum) and human serum albumin are recognized by the common receptor(s) on the cellular membrane in hAdSCs. In addition, the saturable uptake of FITC-albumin in hAdSCs suggested the presence of a receptor molecule that mediates the entry of FITC-albumin into the cells. Based on the Michaelis-Menten equation with a linear term, the K_m value for FITC-albumin uptake in hAdSCs was calculated to be 85.1 μg/ml. The K_m value for FITC-albumin in OK cells was reported to be 24 μg/ml. Zhai et al. (2000) reported that the two receptors, cubilin and megalin, were cooperatively involved in the endocytic uptake of FITC-albumin in OK cells. In contrast, real-time PCR analysis revealed no or very low expression of megalin and cubilin mRNA in hAdSCs employed in this study (data not shown). Further studies are needed to clarify the receptor responsible for albumin uptake in hAdSCs.

The involvement of endocytosis in the cellular entry of FITC-albumin in hAdSCs is supported by the results of various chemical inhibitors (Dutta and Donaldson 2012). The inhibition of FITC-albumin uptake by hAdSCs by 2,4-dinitrophenol, colchicine, and cytochalasin D suggests that the uptake of FITC-albumin requires ATP hydrolysis and polymerization of microtubules and actin, which are essential for endocytic processes. In addition, the inhibitory effects of endosomal acidification inhibitors (chloroquine and bafilomycin A_1) on FITC-albumin uptake in hAdSCs suggest that receptor-mediated endocytosis is involved in the internalization of FITC-albumin because acidification of the endosomal pH is essential for receptor recycling to the cell membrane following the dissociation of the ligand and receptor in the endosome after receptor-mediated endocytosis. The observed inhibitory effects of chloroquine and bafilomycin A_1 were associated with the saturation of FITC-albumin uptake in hAdSCs.

In this study, the expression and subcellular localization of clathrin heavy chain and caveolin-1 in hAdSCs were examined to clarify the involvement of these two proteins in the endocytic uptake of FITC-albumin in hAdSCs. To our knowledge, this is the first report to show the localization of clathrin and caveolin-1 in hAdSCs. Immunofluorescence analysis revealed that clathrin was found in a punctate pattern in the cytoplasm of hAdSCs, indicating the presence of clathrin-coated vesicles (Tebar et al. 1999; Buss et al. 2001). In contrast, caveolin-1 was predominantly detected in the plasma membrane of hAdSCs, indicating the presence of caveolar invaginations on the plasma membrane. It has been reported that caveolin-1 is present on the plasma membrane in MDCK epithelial cells (Dupree et al. 1993; Scheiffele et al. 1998), while diffuse punctate staining has been observed in human bone marrow-derived mesenchymal stem cells (Baker et al. 2012). Although the reasons for the differences in caveolin-1 localization between adipose and bone marrow-derived stem cells is not clear, this may be due to the differences in stem cell tissues and culture conditions.

We found that FITC-albumin uptake was significantly inhibited by both clathrin-dependent endocytosis inhibitors (chloropromazine, phenylarsine oxide, and Pitstop2) and caveolin-dependent endocytosis inhibitors (nystatin and methyl-b-cyclodextrin). Based on these observations, clathrin and caveolin play important roles in the internalization of albumin in hAdSCs. However, it has been pointed out that the results of chemical inhibitors for endocytosis need to be interpreted carefully (Dutta and Donaldson 2012). Therefore, we examined the effects of clathrin and caveolin-1 knockdown on FITC-albumin uptake in hAdSCs. Silencing of clathrin and caveolin-1 was observed by the corresponding siRNA and significantly decreased the uptake of FITC-albumin in hAdSCs. Taken together, FITC-albumin was found to enter hAdSCs through two known routes of entry, namely clathrin-dependent and caveolin-dependent. Yumoto et al. (2006) found that FITC-albumin uptake was mediated by clathrin-dependent endocytosis, but not caveolin-dependent endocytosis, in the cultured alveolar type II epithelial cell line RLE-6TN. In contrast, Dobrinskikh et al. (2014) revealed that caveolin-dependent endocytosis plays a primary role in the internalization of FITC-albumin by human podocytes. Thus, it is likely that the molecular mechanisms underlying the entry of FITC-albumin vary according to the cell type, which may be due to the differences in the albumin-bound receptor(s) expressed in the cell membrane.

In conclusion, we characterized the internalization of FITC-albumin in mesenchymal stem cells from human adipose tissue. The uptake of FITC-albumin in hAdSCs was found to be mediated by both clathrin-dependent and caveolin-dependent endocytosis. Further investigation will be needed to identify the receptor(s) responsible for endocytosis and the physiological roles of the internalization system.

4. Experimental

4.1. Materials

KBM ADSC2 and KBM Trypsin AOF were purchased from Kohjin Bio (Tokyo, Japan). Penicillin-streptomycin solution and Hoechst 33342 were purchased from Life Technologies (Carlsbad, CA, USA). FITC-labeled bovine serum albumin (FITC-albumin), colchicine, phenylarsine oxide, methyl-β-cyclodextrin, and nystatin were purchased from Sigma-Aldrich (St. Louis, MO, USA). 2,4-Dinitrophenol, colchicine, chloroquine, and chlorpromazine were purchased from Nacalai Tesque (Kyoto, Japan). Dynasore was purchased from Tokyo Chemical Industry Co., Ltd. (Tokyo, Japan). Pitstop2 was purchased from Abcam (Cambridge, UK). Clathrin heavy chain siRNA (h) (SC-35067) and caveolin-1 siRNA (h) (SC-29241) were purchased from Santa Cruz Biotechnology (Santa Cruz, CA, USA). All other chemicals used in the experiments were commercial products with the highest purity available.

4.2. Cell culture

Human adipose-derived stem cells (hAdSCs) were purchased from PromoCell GmbH (Heidelberg, Germany). hAdSCs were cultured in KBM ADSC2 solution with 5% fetal bovine serum (FBS) (F7524; Sigma-Aldrich, St. Louis, MO, USA) and 1% penicillin-streptomycin in an atmosphere of 5% CO_2–95% air at 37°C and subcultured every seven days using the detachment solution KBM Trypsin AOF. Fresh medium was replaced every two days. Passages 8–11 were used for the experiments.

4.3. Quantitative uptake study

Cells were grown on 24-well culture plates with KBM ADSC2 solution containing 5% FBS and 1% penicillin-streptomycin. Four days after seeding, the medium was changed to serum-free medium, and the cells were maintained for a further 24 h. After the removal of the culture medium, each well was washed with 1 ml of phosphate-buffered saline (PBS 137 mM NaCl, 3 mM KCl, 8 mM Na_2HPO_4, 1.5 mM KH_2PO_4, 0.1 mM $CaCl_2$, and 0.5 mM $MgCl_2$, pH 7.4) supplemented with 5 mM

D-glucose (PBS-G) in a 37°C water bath. For experiments with a fixed substrate concentration, 0.5 ml of PBS-G containing FITC-albumin (100 µg/ml) was added to each well, and the cells were incubated at 37°C or 4°C for 30, 60, or 120 min. For experiments with various substrate concentrations, 0.5 ml of PBS-G containing FITC-albumin (30, 50, 100, 300, and 500 µg/ml) was added to each well. The cells were preincubated with or without inhibitors for 10 min at 37°C, and then incubated with or without PBS-G containing FITC-albumin (100 µg/ml) at 37°C for 60 min or 120 min. Dimethyl sulfoxide was used as the vehicle at less than 0.5% (v/v) for each control experiment. At the end of the incubation, the uptake buffer was aspirated, and the cells were washed twice with 1 ml of ice-cold PBS. The cells were scraped into 0.5 ml of ice-cold PBS, and the wells were rinsed again with 0.5 ml of ice-cold PBS to improve the recovery of the cells. The cells were further washed by centrifugation at 4°C for 5 min at 10,000 rpm. After the supernatant was aspirated, the pellet was solubilized in 0.2 ml of 0.1% Triton X-100 in PBS at room temperature for 30 min, and then centrifuged for 5 min at 10,000 rpm. The resulting supernatant was used for fluorescence and protein assays.

The amount of FITC-albumin taken up by the cells was measured using an fluorescence spectrophotometer Enspire 2300 (PerkinElmer, Waltham, MA, USA) at an excitation wavelength of 500 nm and an emission wavelength of 520 nm. Protein was determined using the Lowry method with bovine serum albumin as the standard. The half-maximal inhibitory concentration (IC_{50}) values of the inhibitors were calculated using the Hill equation, as previously described (Fujii et al. 2009):

$$A = 100 / [1 + ([I]/IC_{50})^n]$$

where [I] is the concentration of the inhibitor, A is the percentage of FITC-albumin uptake with an inhibitor to that without an inhibitor, and n is the Hill coefficient.

The kinetic parameters for FITC-albumin uptake were calculated using the Michaelis–Menten equation plus linear term (Takano et al. 1994):

$$V = V_{max} [FITC\text{-}albumin] / (K_m + [FITC\text{-}albumin]) + K_d [FITC\text{-}albumin]$$

where V is the uptake rate, [FITC-albumin] is the initial concentration of FITC-albumin, V_{max} is the maximum uptake rate by saturable process, K_m is the Michaelis constant, and K_d is the coefficient of the non-saturable process.

The KaleidaGraph program (Version 4.5, Synergy Software, PA, USA) was used for curve-fitting to the above equations.

4.4. Cell treatment

To examine the effect of inhibitors on FITC-albumin uptake, hAdSCs were preincubated and incubated in the absence or presence of the inhibitors at 37°C. The pretreatment and incubation periods were 10 min and 2 h, respectively. Control cells were treated with the same concentration of dimethyl sulfoxide (DMSO) for each experiment. The concentrations of the inhibitors used in this study were as follows: 2,4-dinitrophenol (1 mM), colchicine (50 µM with 0.5% DMSO), cytochalasin D (5 µM with 0.5% DMSO), chloroquine (100 µM), bafilomycin A_1 (1.6 µM with 0.5% DMSO), chloropromazine (50 µM), phenylarsine oxide (10 µM with 0.5% DMSO), Pitstop2 (30 µM with 0.5% DMSO), nystatin (50 µg/ml in 0.5% DMSO), methyl-β-cyclodextrin (10 mM), and dynasore (80 µM with 0.5% DMSO).

4.5. Confocal microscopy analysis

The cells were grown in 35-mm glass-bottom culture dishes for 24 h. The cells were incubated with FITC-albumin (300 µg/mL) for 120 min at 37°C or 4°C. The cells were then incubated with Hoechst 33342 (10 µM) for 60 min, washed three times with ice-cold PBS, and the fluorescence was visualized by confocal laser scanning microscopy (Zen 2012; Carl Zeiss, Oberkochen, Germany).

For detection of clathrin heavy chain and caveolin-1 expression, the cells were fixed with 4% paraformaldehyde at room temperature for 20 min and permeabilized with 0.25% Triton X-100 in PBS at room temperature for 15 min. After rinsing in PBS, the cells were blocked with 3% normal goat serum (NGS) at room temperature for 1 h with gentle agitation. Afterwards, the cells were incubated overnight at 4°C with purified mouse monoclonal anti-clathrin heavy chain antibody (BD 610499) (1:1,000), or rabbit polyclonal anti-caveolin-1 antibody (ab18199) (1:500) in 3% NGS at 4°C overnight. Finally, the cells were incubated with Alexa Fluor® 488-labeled goat anti-mouse polyclonal antibody (1:1,000) or Alexa Fluor ® 546-labeled goat anti-rabbit polyclonal antibody (1:1,000) at room temperature for 1 h in the dark. After rinsing in PBS, the nuclei were stained with Hoechst 33342 (10 µM) at room temperature for 1 h. The fluorescence was visualized using confocal laser scanning microscopy (Zen 2012; Carl Zeiss).

4.6. Western blotting

For immunoblot analysis of clathrin heavy chain and caveolin-1 in hAdSCs, whole cell lysates were prepared 7 days after seeding. After removal of the culture medium, the cells were washed and collected in PBS with a cell scraper. The cell suspension was centrifuged at 3,000 rpm at 4°C for 5 min. After the supernatant was discarded, the cells were lysed with PBS containing 1% (v/v) Triton X-100, 0.1% (w/v) SDS, and 1% (w/v) deoxycholic acid. The cell lysates were vortexed and incubated on ice for 30 min. The supernatant was collected by centrifugation at 10,000 rpm at 4°C for 5 min and used as a sample for immunoblotting. The samples were separated on 10% polyacrylamide gels by SDS-PAGE and transferred onto nitrocellulose membranes, as described previously. The membranes were blocked with 3% (w/v) bovine serum albumin (BSA) in PBS containing 0.1% Tween-20 (3% BSA-PBST) at room temperature for 1 h and immunoblotted with purified mouse monoclonal anti-clathrin heavy chain antibody (610499; BD Biosciences) (1:1,000), rabbit polyclonal anti-caveolin-1 antibody (ab18199; Abcam) (1:500), and mouse monoclonal anti-β-actin antibody (A2228; Sigma) (1:5,000) in 3% BSA-PBST at room temperature for 1 h or at 4°C overnight. The membranes were then washed three times with PBST for 5 min each and incubated with horseradish peroxidase-conjugated anti-rabbit or mouse IgG antibody in 5% (w/v) non-fat dry milk in PBST at room temperature for 1 h. After the membranes were washed with PBST three times, immunoreactive bands were detected using Amersham ECL chemiluminescent reagent (GE Healthcare Bio-Sciences, Piscataway, NJ, USA) and Amersham Imager 600 (Cytiva, Tokyo, Japan). Band intensities were quantified after background correction using ImageJ software.

4.7. siRNA knockdown study

The cells were seeded in a 6-well tissue culture plate at a density of 3×10^5 cells per well in 2 ml of antibiotic-free normal growth medium supplemented with FBS. The plate was incubated at 37°C in a CO_2 incubator until the cells reached 60-80 % confluent. The siRNA solution (clathrin heavy chain siRNA, 100 nM; caveolin-1 siRNA, 50 nM) in Opti-MEM (Thermo Fisher Scientific, Waltham, MA, USA) was mixed with Lipofectamine 2000 (Thermo Scientific Waltham, MA, USA) and added to each well. The plate was shaken gently to mix the solution, and the transfected cells were incubated for 4 h at 37°C in a CO_2 incubator. The transfection mixture was then removed and replaced with serum-free normal growth medium (KBM ADSC2 solution with 1% penicillin-streptomycin). The cells were incubated for an additional 48 h in an atmosphere of 5% CO_2 and 95% air at 37°C. The cells were then used for the uptake study and western blotting.

4.8. Statistical analysis

Data are expressed as the mean ± standard error (S.E.). Statistical analysis was performed using Student's t-test or Tukey's HSD test for multiple comparisons. Statistical significance was set at $P < 0.05$.

Acknowledgements: This work was supported in part by JSPS KAKENHI (grant no. 19K07235 and 20K16096).

Competing interest: The authors declare no competing interests.

References

Baker N, Zhang G, You Y, Tuan RS (2012) Caveolin-1 regulates proliferation and osteogenic differentiation of human mesenchymal stem cells. J Cell Biochem 113: 3773–3787.

Buss F, Arden SD, Lindsay M, Luzio JP, Kendrick-Jones J (2001) Myosin VI isoform localized to clathrin-coated vesicles with a role in clathrin-mediated endocytosis. EMBO J 20: 3676–3684.

Chulpanova DS, Kitaeva KV, Tazetdinova LG, James V, Rizvanov AA, Solovyeva VV (2018) Application of mesenchymal stem cells for therapeutic agent delivery in anti-tumor treatment. Front Pharmacol 9: 259.

Conner SD, Schmid SL (2003) Regulated portals of entry into the cell. Nature 422: 37–44.

Dobrinskikh E, Okamura K, Kopp JB, Doctor RB, Blaine J (2014) Human podocytes perform polarized, caveolae-dependent albumin endocytosis. Am J Physiol Renal Physiol 306: F941–F951.

Dupree P, Parton RG, Raposo G, Kurzchalia TV, Simons K (1993) Caveolae and sorting in the trans-Golgi network of epithelial cells. EMBO J 12: 1597–1605.

Dutta D, Donaldson JG (2012) Search for inhibitors of endocytosis: intended specificity and unintended consequences. Cell Logist 2: 203–208.

Fujii K, Nagai J, Sawada T, Yumoto R, Takano M (2009) Effect of pegylation of N-WASP181-200 on the inhibitory potency for renal aminoglycoside accumulation. Bioconjug. Chem. 20: 1553–1558.

Gao Z, Zhang L, Hu J, Sun Y (2013) Mesenchymal stem cells: a potential targeted-delivery vehicle for anti-cancer drug, loaded nanoparticles. Nanomedicine 9: 174–184.

Hsu SH, Ho TT, Tseng TC (2012) Nanoparticle uptake and gene transfer efficiency for MSCs on chitosan and chitosan-hyaluronan substrates. Biomaterials 33: 3639–3650.

Kern S, Eichler H, Stoeve J, Klüter H, Bieback K (2006) Comparative analysis of mesenchymal stem cells from bone marrow, umbilical cord blood, or adipose tissue. Stem Cells 24: 1294–1301.

Kunze KN, Burnett RA, Wright-Chisem J, Frank RM, Chahla J (2020) Adipose-derived mesenchymal stem cell treatments and available formulations. Curr. Rev. Musculoskelet. Med. 13: 264–280.

Lin Y, Liu L, Li Z, Qiao J, Wu L, Tang W, Zheng X, Chen X, Yan Z, Tian W (2006) Pluripotency potential of human adipose-derived stem cells marked with exogenous green fluorescent protein. Mol Cell Biochem 291: 1–10.

Lindvall O, Kokaia Z, Martinez-Serrano A (2004) Stem cell therapy for human neurodegenerative disorders-how to make it work. Nat Med 10 Suppl: S42–S50.

Lowry OH, Rosebrough NJ, Farr AL, Randall RJ (1951) Protein measurement with the Folin phenol reagent. J Biol Chem 193: 265–275.

Miaczynska M, Stenmark H (2008) Mechanisms and functions of endocytosis. J Cell Biol 180: 7–11.

Scheiffele P, Verkade P, Fra AM, Virta H, Simons K, Ikonen E (1998) Caveolin-1 and –2 in the exocytic pathway of MDCK cells. J. Cell Biol 140: 795–806.

Schwegler JS, Heppelmann B, Mildenberger S, Silbernagl S (1991) Receptor-mediated endocytosis of albumin in cultured opossum kidney cells: a model for proximal tubular protein reabsorption. Pflugers Arch 418: 383–392.

Scioli MG, Storti G, D'Amico F, Gentile P, Kim BS, Cervelli V, Orlandi A (2019) Adipose-derived stem cells in cancer progression: new perspectives and opportunities. Int J Mol Sci 20: 3296.

Segers VF, Lee RT (2008) Stem-cell therapy for cardiac disease. Nature 451: 937–942.

Shah K (2012) Mesenchymal stem cells engineered for cancer therapy. Adv Drug Deliv Rev 64: 739–748.

Strem BM, Hicok KC, Zhu M, Wulur I, Alfonso Z, Schreiber RE, Fraser JK, Hedrick MH (2005) Multipotential differentiation of adipose tissue-derived stem cells. Keio J Med 54: 132–141.

Takano M, Ohishi Y, Okuda M, Yasuhara M, Hori R (1994) Transport of gentamicin and fluid-phase endocytosis markers in the LLC-PK1 kidney epithelial cell line. J Pharmacol Exp Ther 268: 669–674.

Tebar F, Bohlander SK, Sorkin A (1999) Clathrin assembly lymphoid myeloid leukemia (CALM) protein: localization in endocytic-coated pits, interactions with clathrin, and the impact of overexpression on clathrin-mediated traffic. Mol Biol Cell 10: 2687–2702.

Yang Y, Wang Q, Song L, Liu X, Zhao P, Zhang F, Gu N, Sun J (2017) Uptake of magnetic nanoparticles for adipose-derived stem cells with multiple passage numbers. Sci China Mater 60: 892–902.

Yumoto R, Nishikawa H, Okamoto M, Katayama H, Nagai J, Takano M (2006) Clathrin-mediated endocytosis of FITC-albumin in alveolar type II epithelial cell line RLE-6TN. Am J Physiol Lung Cell Mol Physiol 290: L946–L955.

Zhai XY, Nielsen R, Birn H, Drumm K, Mildenberger S, Freudinger R, Moestrup SK, Verroust PJ, Christensen EI, Gekle M (2000) Cubilin- and megalin-mediated uptake of albumin in cultured proximal tubule cells of opossum kidney. Kidney Int. 58: 1523–1533.

Zhang J, Liu Y, Chen Y, Yuan L, Liu H, Wang J, Liu Q, Zhang Y (2020) Adipose-derived stem cells: current applications and future directions in the regeneration of multiple tissues. Stem Cells Int. 2020: 8810813.

Zuk PA, Zhu M, Mizuno H, Huang J, Futrell JW, Katz AJ, Benhaim P, Lorenz HP, Hedrick MH (2001) Multilineage cells from human adipose tissue: implications for cell-based therapies. Tissue Eng 7: 211–228.

Zuk PA, Zhu M, Ashjian P, De Ugarte DA, Huang JI, Mizuno H, Alfonso ZC, Fraser JK, Benhaim P, Hedrick MH (2002) Human adipose tissue is a source of multipotent stem cells. Mol Biol Cell 13: 4279–4295.